



## ORIGINAL ARTICLE

# Green approach to synthesize nano zinc oxide via *Moringa oleifera* leaves for enhanced anti-oxidant, anti-acne and anti-bacterial properties for health & wellness applications



Nitesh Bhalla<sup>a,b,\*</sup>, Nitin Ingle<sup>b</sup>, Athira Jayaprakash<sup>b</sup>, Hiral Patel<sup>b</sup>,  
Srilakshmi V. Patri<sup>a</sup>, D. Haranath<sup>c</sup>

<sup>a</sup> Department of Chemistry, National Institute of Technology, Warangal 506004, Telangana, India

<sup>b</sup> IFFCO Group, Seville Products LLC, Plot 24, Street 3B, Umm Ramool, PO Box 10596, Dubai, UAE

<sup>c</sup> Department of Physics, National Institute of Technology, Warangal 506004, Telangana, India

Received 10 August 2022; accepted 5 December 2022

Available online 9 December 2022

## KEYWORDS

Green synthesis ZnO  
Nanoparticles (GsZnO-Nps);  
Advance Antibacterial effi-  
cacy;  
Anti-oxidant efficacy;  
Anti-acne efficacy;  
Free Radical Scavenging  
Potency (FRSP);  
Health and wellness  
application

**Abstract** This article explores green synthesis as a strategic and sustainable route to fabricate potent zinc oxide nanoparticles. Natural green based antibacterial agents and alternatives are being introduced in the market however there is a dearth in green approach moringa based zinc oxide nanoparticles in personal care products and establishing efficacy. *Moringa oleifera* comprises various phytochemicals that act as non-toxic stabilizing and reducing agents. Green synthesized ZnO nanoparticles (GsZnO-Nps) were investigated for their morphological and physicochemical properties using various advanced characterizing techniques. The hexagonal wurtzite structure of GsZnO-Nps is determined by X-ray diffractometry (XRD), the average crystallite size is 13.82 nm, total crystallinity was 95.91 % and high specific-surface-area is 77.38 m<sup>2</sup>/g. Scanning Electron Microscope (SEM) revealed the formation of spherical nanoparticles having a diameter of 50 nm. UV-vis spectrum shows high bandgap energy of 3.36 eV. Results have shown that antioxidant efficacy of GsZnO-Nps is significantly higher than AR-Grade ZnO, evaluated by using 2, 2-diphenyl-1-picrylhydrazyl (DPPH) assay. Half-maximal inhibitory concentration (IC<sub>50</sub>) of GsZnO-Nps was 21.72 µg/mL and AR-Grade ZnO was 345.57 µg/mL. GsZnO-Nps (0.0183 g/mL) shows robust anti-acne efficacy against *Cutibacterium acne* (*C. acne*) organism which estimated by ZOI technique, have average ZOI of 33 mm, with standard error 0.577 mm. Antibacterial efficacy of GsZnO-Nps

\* Corresponding author.

E-mail address: bhalla.nitesh@gmail.com (N. Bhalla).

Peer review under responsibility of King Saud University.



Production and hosting by Elsevier

was established at different concentrations (10, 50, 100, and 200  $\mu\text{g}/\text{mL}$ ) against Gram-positive and Gram-negative pathogens by zone-of-inhibition (ZOI) method with respect to standard drugs. GsZnO-Nps at 200  $\mu\text{g}/\text{mL}$  exhibits high ZOI of 26.75 mm against *Escherichia coli* (*E. coli*) and ZOI of 30 mm against *Staphylococcus aureus* (*S. aureus*) organisms respectively which is comparatively higher or equal to standard drugs. The minimum inhibitory concentration (MIC) of GsZnO-Nps is 500  $\mu\text{g}/\text{mL}$  to inhibit the microbe's growth. GsZnO-Nps established the added benefits of moringa phytochemicals and is an excellent approach to developing eco-friendly and multi-functional versatile products having strong antioxidants, anti-acne and advanced antibacterial efficacy for numerous industrial applications like cosmetic, health hygiene products, drugs, therapeutic etc.

© 2022 The Author(s). Published by Elsevier B.V. on behalf of King Saud University. This is an open access article under the CC BY-NC-ND license (<http://creativecommons.org/licenses/by-nc-nd/4.0/>).

## 1. Introduction

Nanotechnology and nanoscience have seen a tremendous increase in industrial applications in the past decade. Plant-based synthesis of nanoparticles is a unique approach that has various applications in cosmetics, medicine, food, and agriculture industries (Malik et al., 2014; Kalpana and Rajeswari, 2018; Singh et al., 2008; Bhalla et al., 2022; Bhalla et al., 2022). *Moringa oleifera* tree also known as drumstick tree is native to Asia particularly India and also grown in the Philippine, Sudan, Egypt, and South Africa. It is a member of the *Moringa* species and the *Moringaceae* family, and is renowned for its safe to eat soft beans, flowers and leaves. The leaves, notably, are well-known for their prophylactic and therapeutic powers and are often devoured in meals. Extracts obtained from the leaves have powerful antioxidant capabilities and high antibacterial action against Gram-positive and Gram-negative bacteria. Additionally, phytochemicals in *Moringa oleifera* leaves show incredible properties such as anti-cancer, anti-inflammatory, anti-diabetics and are suitable for applications in different industries such as foodstuff, cosmetics, and drug delivery (Bhalla et al., 2021).

Drug delivery, nanomedicine, gene delivery and biosensing are the new horizon of the nanoscience field (Jianrong et al., 2004; Zhang et al., 2009). Plant-derived methods using such biological agents help in stabilizing and reducing particles into nano scale having a high shelf life. The plant-based synthesis methods have inherent variability due to the presence of several phytochemicals like phenolic compounds, flavonoids, vitamins, and carbohydrates. These phytochemicals contain amine, carbonyl, and hydroxyl functional groups which help in the reduction of metals ions and convert them into nano-scale particles (Makarov, 2014; Arya, 2010). However, it has been seen that most favorably phenolic and flavonoid-containing functional groups play a vital role in the green synthesis of nanoparticles (Biswas et al., 2013; Virkutyte and Varma, 2011). Green synthesized nanomaterials are found to be non-toxic, cost-effective and biodegradable in nature (Nadagouda and Varma, 2008; Darroudi et al., 2014; Irvani, 2011; Behravan et al., 2019). Being an eco-friendly approach, the green synthesis method helps to reduce the consumption of hazardous chemicals and use natural materials such as roots, leaves, flower, bark extract and even microbes like algae, fungus, bacteria, etc. (Rajiv et al., 2013; Menazea et al., 2021; Moodley et al., 2018). Recent literatures show the importance of nanoparticles of metal and their oxides synthesized by green route like zinc, silver, copper, nickel, gold, etc. (Singh, et al., 2021; Suresh et al., 2018; Sushma et al., 2016).

ZnO is commonly generally recognized as safe and shows a high potential to kill the disease-causing germs in humans and animals (Kołodziejczak-Radzimska and Jesionowski, 2014; Anter, 2020; Iqbal et al., 2021). The high specific surface area of the nanoparticles and phytochemicals of plants shows the remarkable and exclusive

properties which can play a very important role in their antibacterial, anti-oxidant and photocatalytic application (Kolekar et al., 2013; Zheng et al., 2015; Yedurkar et al., 2016; Abd El-Kader et al., 2021).

Numerous routes to synthesize ZnO nanoparticles have been reported in the literature, the non-basic route (Oprea et al., 2011), high energy ball mills technique (Wirunchit et al., 2021), combustion route (Vasile et al., 2012), vaporization (Sánchez-Martín et al., 2021), assembly assisted (Goktas and Goktas, 2021) and sol-gel technique (Hasnidawani et al., 2016), etc. However, certain drawbacks of these synthesis methods of nano ZnO are: high energy consumption, time, cost, labor-intensive, solvents used, and byproducts released are not permissible in most industrial applications. Moreover, nanoparticles synthesized using chemical methods have limited opportunity for medicinal sector applications due to their possible toxicity and harmful byproducts. Hence, the present study explores eco-friendly and sustainable method which is suitable for different industrial applications.

In recent times there are huge challenges in evolving and innovating strong antibacterial agents. As per the last 5 years, the Food and Drug Administration (FDA) have banned the most common antimicrobial agent like triclosan, triclocarban, and 18 others from the personal care industry (Halden, 2014). This action was taken due to major apprehensions about the carcinogenic effects, cell toxicity of these materials on the environment, humans and wildlife. Recently, in 2021 the European Commission declared Zinc Pyrithione (ZPT) well known antifungal agent as a prohibited ingredient due to its cell toxicity (Lamore et al., 2010). Moreover, microbes no longer respond to existing germicidal agents because of mutations and resistant built against them. As a result, novel, natural, strong antimicrobial agents are extremely required for the home and personal care industry.

In our previous research article, we have reported 25 phytochemicals in aqueous *Moringa oleifera* leaf extract evaluated by GC-MS along with their free radicle scavenging potency (Bhalla et al., 2021). *Moringa oleifera* leaves extract acts as a biodegradable, natural and non-toxic reducing agent for fabrication of nano-scale ZnO. The evaluation and characterizations of GsZnO-Nps are done by using advanced technical tools like UV Vis, FTIR, XRD, SEM-EDX. Moreover, the antioxidant of GsZnO-Nps and AR Grade ZnO has been evaluated using 2,2-diphenyl-1-picrylhydrazyl (DPPH) standard free radical. The  $\text{IC}_{50}$  concentration GsZnO-Nps was significantly lower than AR-Grade ZnO.

This may be the first or among the very few researches that have established the potency of green synthesized zinc oxide using moringa leaves extract against *C. acne* and additionally demonstrated efficacy equivalent to standard drugs with respect to *S. aureus* and *E. coli* bacterium. The present research work mainly aims on reporting eco-friendly and sustainable methods of green synthesized ZnO nanoparticles (GsZnO-Nps) using *Moringa oleifera* leaves for addressing the rapidly growing needs of advanced antibacterial and anti-oxidant agent for health & wellness applications. This research will further

help to increase the application of green synthesized versatile nano-materials in the medicine, health & wellness, cosmetic, personal care sector.

## 2. Materials and methods

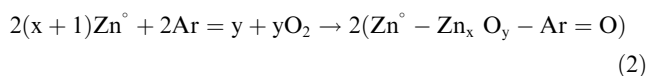
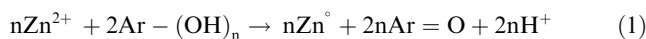
### 2.1. Materials

Zinc Acetate 99.5 % ( $C_4H_6Zn \cdot 2H_2O$ ) from S D Fine-chem limited, Mumbai, India. *Moringa oleifera* leaves powder from Holy Natural, India. Extra pure 2,2-Diphenyl-1-Picrylhydrazyl (DPPH) from SRL Pvt. Ltd. Distilled water having pH 5.5–7.0 &  $1\mu S/cm$  conductivity. Bacterial cultures *E. coli* ATCC 10536, *C. acne* ATCC 11,827 and *S. aureus* ATCC 6538 were purchase through ATCC bank (American Type of Culture Collection) and standard drugs (Doxycycline, Azithromycin, Cefpodoxime) from local pharmacies.

### 2.2. Method of green synthesis ZnO nanoparticles

Prepare decoction of *Moringa oleifera* leaves powder with distilled water at 1:20 ratio under continuous stirring at 80–90 °C for 6 h. Filter the above mixture using Whatman filter paper-1 to get separated solid leaf pieces from the *Moringa oleifera* leaves extract. Add 0.272 mol of zinc acetate dihydrate (final concentration in mixture to be 0.0597 g/mL) to the filtered plant extract with continuously stirring for 2–3 h at 80–90 °C until precipitation is observed. Set the solution aside for 18 h in room temperature in order to facilitate the reaction completion and formation of ZnO nanoparticles. A dark green mixture having a pH of 7.45 and settled precipitates is observed. Centrifuge the solution at 3000 rpm to collect

GsZnO-Nps and dry at 50 °C to make it powder for further evaluation Fig. 1. The possible mechanism of green synthesis of nano ZnO formation, using herbal extract is described as,



The phytochemicals such as phenolic compounds and flavonoids ( $Ar-(OH)_n$ ) present in *Moringa oleifera* leaves extract are responsible for synthesis of GsZnO-Nps. ( $Ar-(OH)_n$ ) losses an electron.

for the reduction of  $Zn^{2+}$  to  $Zn^{\circ}$  and possible formation of  $Zn^{\circ}$ -phenolate complex by chelation effect which helps in the synthesis of ZnO nanoparticle at 80–90 °C (Hasan et al., 2021).

### 2.3. Characterizations

UV–Visible spectrum was recorded by using UV–vis spectrophotometer Model-1800 from Shimadzu, Japan. The suspension of GsZnO-Nps and AR Grade ZnO was prepared in distilled water and sonicated for 10 min before measuring the UV–vis spectra. The absorbance range of ZnO was 200–700 nm. FT-IR spectrums were recorded by using FT-IR Spectrophotometer Model- IR Affinity-1S (Shimadzu) Japan. ATR (Attenuated Total Reflection) from SPECAC, U.K. in the wavelength of 4000–400  $cm^{-1}$ . The crystallization properties, size, and phase analysis of GsZnO-Nps were examined by using an X-ray diffractometer (XRD Shimadzu-6100) having scanning range  $2\theta$ , degree 20°–70°, CuK1 radiation ( $\lambda = 1.54056 \text{ \AA}$ ), voltage 40 kV and current 30 mA. The surface mor-

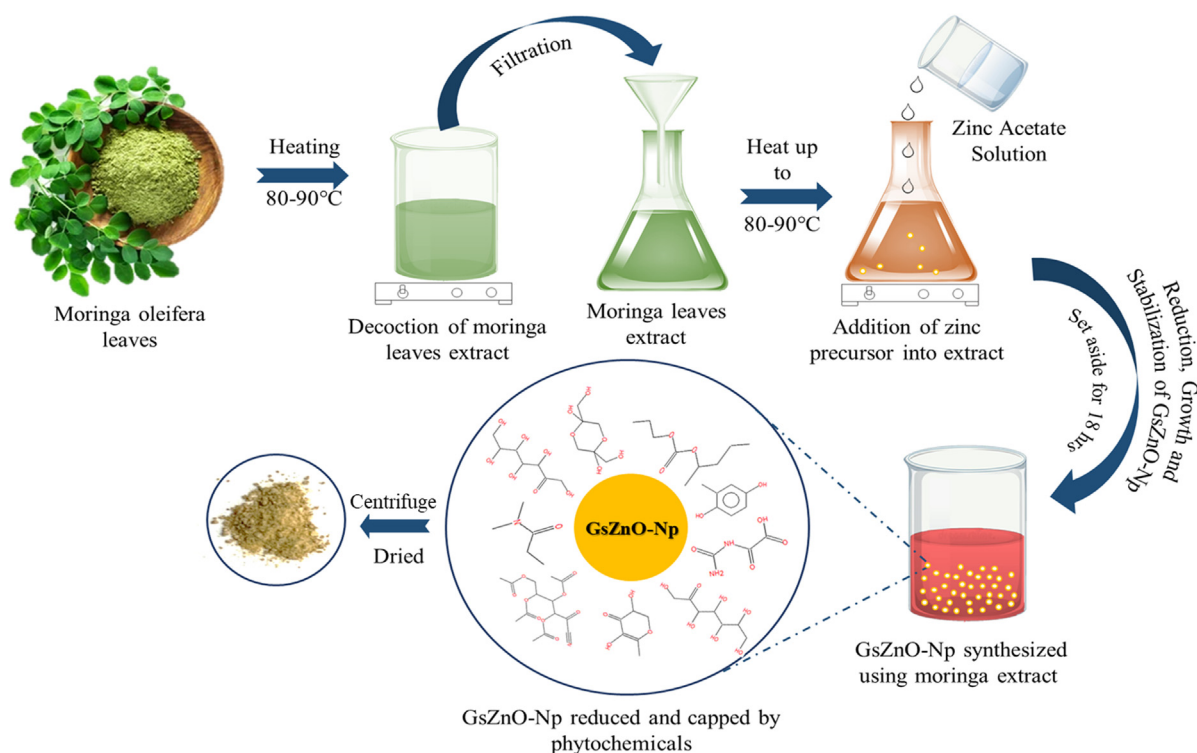


Fig. 1 Systematic presentation of synthesis of GsZnO-Nps via *Moringa oleifera* leaves.

phology of green synthesis ZnO nanoparticles (GsZnO-Nps) was explored by using SEM Model-JSM-6010 PLUS ILA. The range magnification was x50k to x100k, parameter 10 kV, WD 12 mm. The qualitative and quantitative elemental analysis was assessed by Energy Dispersive X-ray Spectroscopy (EDS).

#### 2.4. Anti-oxidant efficacy

The anti-oxidant efficacy of GsZnO-Nps has been determined by using the DPPH assay. Methanolic solution of  $1.52 \times 10^{-4}$  M of DPPH was used in 1:1 ratio with GsZnO-Nps at varying concentrations. anti-oxidant efficacy percentage was examined after incubating the mixture of GsZnO-Nps with DPPH for 30 min and recording the absorption at 517 nm. The half-maximal inhibitory concentration ( $IC_{50}$ ) is measured to study the antioxidant potency of nanoparticles to reduce the DPPH. The control samples were prepared using DPPH solution and mixed only with respective solvents (aqua/methanol) at a 1:1 ratio and measured at 517 nm, the same method followed which was reported in the previously published literature (Bhalla et al., 2021).

$$\text{Antioxidant efficacy \%} = \frac{\text{Control (abs)} - \text{Sample (abs)}}{\text{Control (abs)}} \times 100 \quad (3)$$

#### 2.5. Anti-acne efficacy

GsZnO-Nps were studied for the anti-acne efficacy against *C. acne* using disk diffusion technique commonly known as Kirby Baurer method. This is a qualitative technique to test the ability of a material to inhibit microbial growth by measuring ZOI. Overnight bacterial culture was grown at 37 °C and its cell density was adjusted to  $10^8$  cfu/mL (i.e. Optical density of 0.1 at 600 nm). 0.1 mL of bacterial culture was spread onto sterile Muller Hinton agar plates. Plates were allowed to dried followed by placing 6 mm sterile disc soaked for 30 min in GsZnO-Nps and Zinc acetate concentration 0.0183 g/mL. Post incubation at 37 °C for 24 h, ZOI around the disc was measured.

#### 2.6. Antibacterial activity

The same disk diffusion technique (section 2.5) was used for determination of the antibacterial efficacy against *S. aureus* and *E. coli* (both of  $10^8$  cfu/mL). 6 mm sterile disc soaked for 30 min in different concentrations of GsZnO-Nps, AR Grade ZnO and standard drugs were used for study. Post incubation at 37 °C for 24 h, ZOI around the disc was measured.

Minimum inhibitory concentration of GsZnO-Nps against Gram-positive and Gram-negative pathogens were determined by agar dilution method. Stock solution of GsZnO-Nps was diluted using Muller Hinton agar to achieve a final concentration of 900, 700, 500, 300, 100 µg/mL. Mixture was vortex well and pour onto sterile petri plate and allowed to solidify. After solidification,  $10^8$  cfu/mL of saline suspension of test organisms *E. coli* and *S. aureus* were streaked on every plate and incubated at 37 °C for 48 h. Inhibition of growth was judged by comparison with growth in control plates. The MIC was

defined as the lowest concentration of particles that showed no visible growth after incubation (Siddiqi et al., 2018).

### 3. Results and discussion

#### 3.1. UV-vis spectrum

The UV-Visible absorption spectrum of GsZnO-Nps and AR grade ZnO was examined by a UV-vis spectrophotometer in the range of 200–700 nm. The AR Grade ZnO exhibits the absorption peak at 386 nm with an energy bandgap of 3.20 eV correspondingly GsZnO-Nps exhibits a typical absorption peak in the UV range at 368.5 nm having bandgap energy of 3.36 eV shown in Fig. 2 (A and B).

Based on UV wavelength, the band gap (Eg) was calculated with formula (Bhalla et al., 2022):

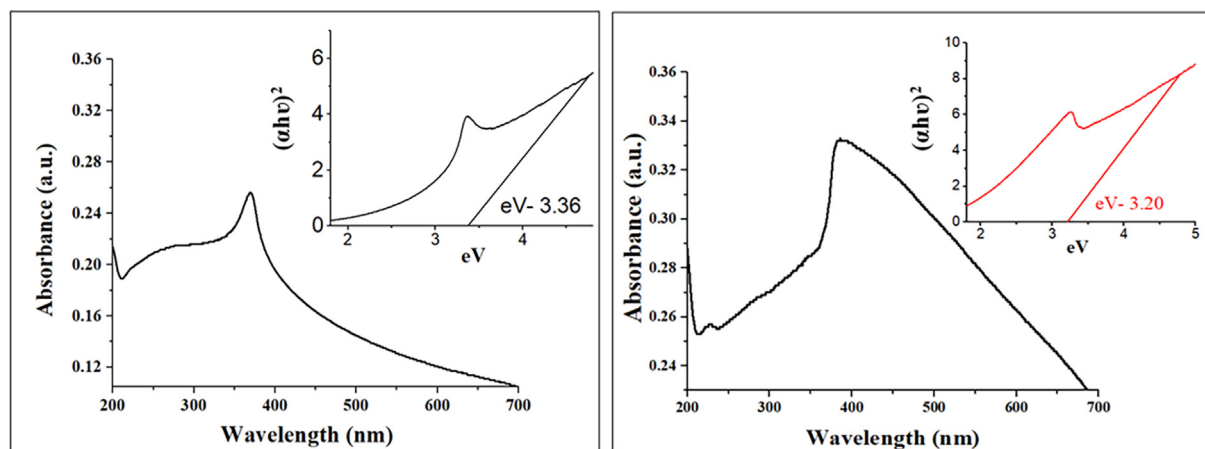
$$E = h \frac{c}{\lambda} \quad (4)$$

where:  $h = 6.626 \times 10^{-34}$  Joules *sec* is the Planks constant,  $c = 3.0 \times 10^8$  m/s is the speed of light and  $\lambda$  is the wavelength.

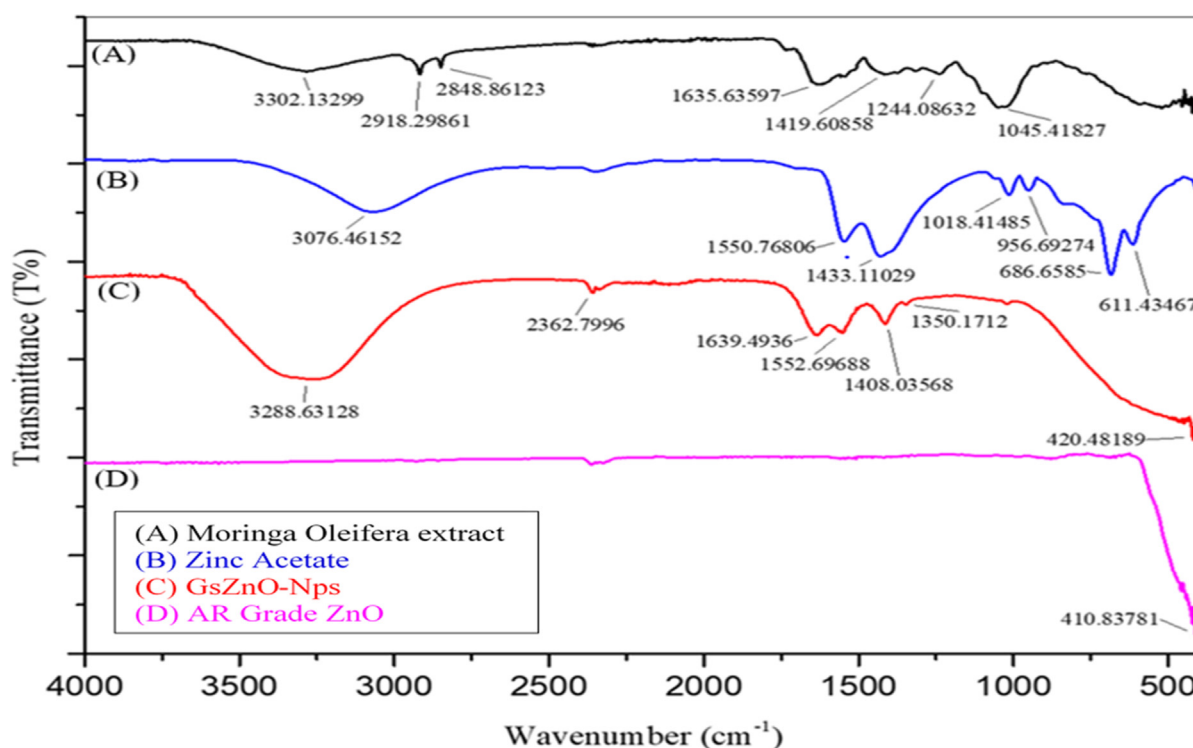
The high band gap energy of GsZnO-Nps clearly indicate the successful synthesis of nanoparticles. A blue shift of absorption bands was observed in the GsZnO-Nps spectra unlike bulk AR grade ZnO. The blue shift could be because of several reasons, like the quantum confinement effect explaining the bandgap energy inversely proportional to particle size, and shows a blue shift as the particle size decreases. The particle size decreases and approaches the size of the electron-hole distance, particle energy levels become quantum confined and separate thus confining the motion of the electron (Debanath and Karmakar, 2013).

#### 3.2. Fourier-transform infrared spectroscopy (FT-IR)

IR spectrum of moringa extract and GsZnO-Nps exhibits the functional group in different regions as shown in Fig. 3. Spectrum (A, B, and C) shows the sharp broad peak in the single bond region with a shift from 3076.63 to 3302.13  $\text{cm}^{-1}$  suggests the existence of the hydroxyl (OH) group which can be attributed to the presence of H<sub>2</sub>O molecules. Spectrum (A) shows the two peaks at 2918.29  $\text{cm}^{-1}$  and 2848.86  $\text{cm}^{-1}$  could be due to symmetrical and asymmetrical C–H stretching of phytochemicals (Joshi et al., 2022). Small peak at 2362.79  $\text{cm}^{-1}$  observed Spectrum (C) could be due to O=C=O stretching probably due to the impurity during synthesis or measuring condition (Bhalla et al., 2022). The peak at 1635.63  $\text{cm}^{-1}$  and 1639.49  $\text{cm}^{-1}$  in spectrum (A & C) could be attributed to the stretching of (C=C) group of phenolic compounds (Joshi et al., 2022). The peaks at 1550.76, 1552.69 and 1350.17  $\text{cm}^{-1}$  in spectrum (B & C) could be due to asymmetrical and symmetrical stretching bonds of COO<sup>-</sup> (Hasan et al., 2021). Peak at 1408.03 to 1433.11  $\text{cm}^{-1}$  in spectrum (A, B & C) could be attributed to the –C–H bending vibration. The peaks 1244.08  $\text{cm}^{-1}$  could be C–O stretching vibration. While 1045.41  $\text{cm}^{-1}$  peak is the due to the C-OH bending of carbohydrates present in moringa extract. The peak 1018.41  $\text{cm}^{-1}$  in spectrum B could be due to C-CH<sub>3</sub> framework originated from zinc acetate (Phoohinkong et al., 2017). While the peak at 956.69  $\text{cm}^{-1}$  exhibit the existence of vinyl C–H out-of-plane bend. The peak at 686.65 and 611.43  $\text{cm}^{-1}$  could



**Fig. 2** The UV-vis absorption spectrum and band gap energy of (A) GsZnO-Nps (B) UV-vis spectrum AR grade ZnO given for comparative study.



**Fig. 3** FT-IR spectrum of (A) *Moringa oleifera* leaves powder (B) Zinc acetate (C) GsZnO-Nps (D) AR Grade Zinc oxide in the spectral range of 400–4000  $\text{cm}^{-1}$ .

be due to out-of-plane bend of OH vibration. Spectrum (C and D) shows the peaks at  $420.48 \text{ cm}^{-1}$  and  $410.83 \text{ cm}^{-1}$  indicating the presence of ZnO similar to previously reported literatures. (Bechambi et al., 2015; Hasan et al., 2021).

### 3.3. X-ray diffraction analysis

The crystalline structure of GsZnO-Nps was analyzed by an X-ray diffractometer. The diffractogram confirms the hexagonal wurtzite structure of GsZnO-Nps (Lei et al., 2012). The diffraction peaks were found at  $2\theta$  values of  $31.53^\circ$ ,  $34.19^\circ$ ,  $36.02^\circ$ ,  $47.31^\circ$ ,  $56.37^\circ$ ,  $62.63^\circ$ ,  $66.16^\circ$ ,  $67.72^\circ$ , and  $68.86^\circ$ . These

peaks are in line with JCPDS standard card 36–1451 of ZnO shown in Fig. 4 (A, B and C) which is in line with previously published literatures [4, 5 and 17]. The average crystallites size of GsZnO-Nps is 13.82 nm (Table 1) which is significantly lower than AR Grade ZnO is 30.87 nm and other previous reported literature (Jayachandran et al., 2021). Debye-Scherrer equation was used for evaluation of crystallite size,

$$D = K\lambda/\beta \cos \theta \quad (5)$$

D- Crystallites size,  $\lambda$ - The wavelength of X-ray, K-Scherrer constant (0.9),  $\theta$ -Braggs angle in radians and  $\beta$ -Full width at half maxima of the peak in radians.

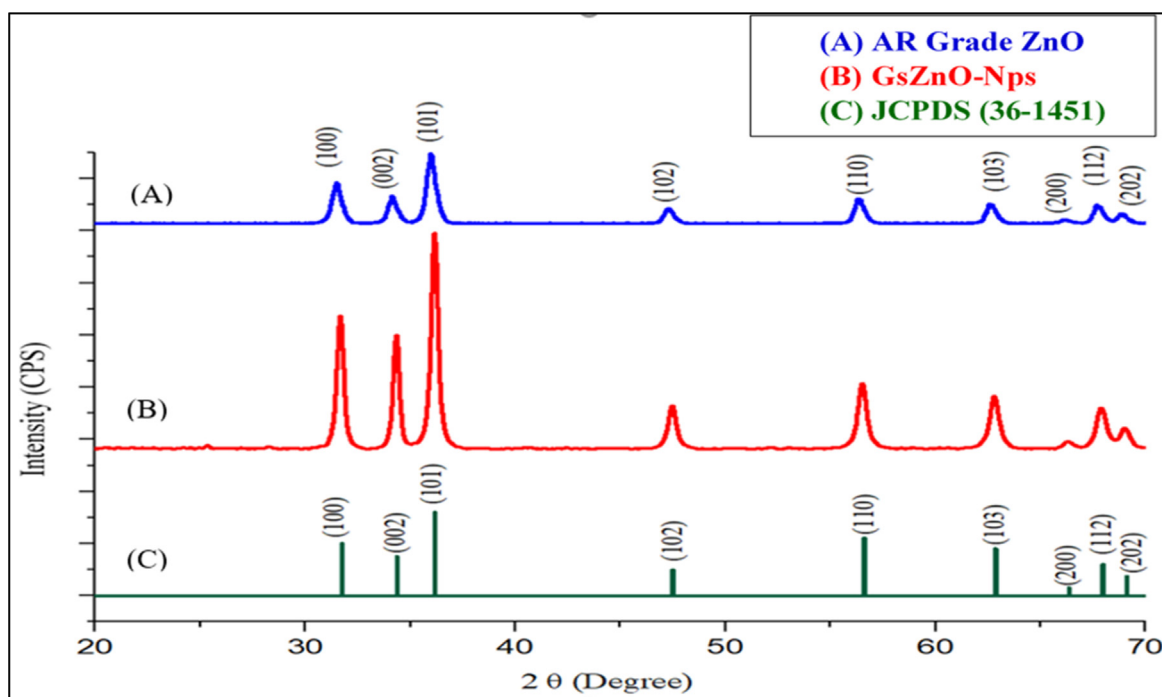


Fig. 4 XRD spectrum of (A) AR Grade ZnO (B) GsZnO-Nps and (C) JCPDS Standard card no. 36-1451 given for reference.

**Table 1** Average crystalline size, Total crystallinity and specific surface area of GsZnO-Nps and AR grade ZnO.

Name of materials	Average crystallite size (nm)	Total crystallinity (%)	Specific surface area (m <sup>2</sup> /g)
GsZnO-Nps	13.82	95.91	77.38
AR Grade ZnO	30.87	95.50	42.64

### 3.3.1. Specific surface area

Specific surface area is the property of solid materials which measure total surface area per unit mass of bulk volume, solid or cross-sectional area. The specific surface area can be evaluated by using the following equation,

$$S = 6 \times 10^3 / D_p \times \rho \quad (6)$$

where S- specific surface area,  $D_p$  – particle size (average crystallite),  $\rho$ - density of ZnO 5.61 g/cm<sup>3</sup>.

The Specific surface area of GsZnO-Nps and AR Grade ZnO was found to be 77.38 m<sup>2</sup>/g and 42.64 m<sup>2</sup>/g. GsZnO-Nps has significantly higher specific surface area than AR Grade ZnO as well as nano ZnO in other reported literature (Jayachandran et al., 2021). The specific area can play important role in the antibacterial efficacy due to high surface availability and destruction of the cell wall of microorganisms.

### 3.3.2. Total crystallinity

The total crystallinity of GsZnO-Nps and AR Grade ZnO was found to be 95.91 % and 95.50 % respectively calculated by following equation,

$$\text{Total crystallinity \%} = \frac{\text{Area of crystalline peaks}}{\text{Area of total peaks (crystalline + amorphous)}} \times 100 \quad (7)$$

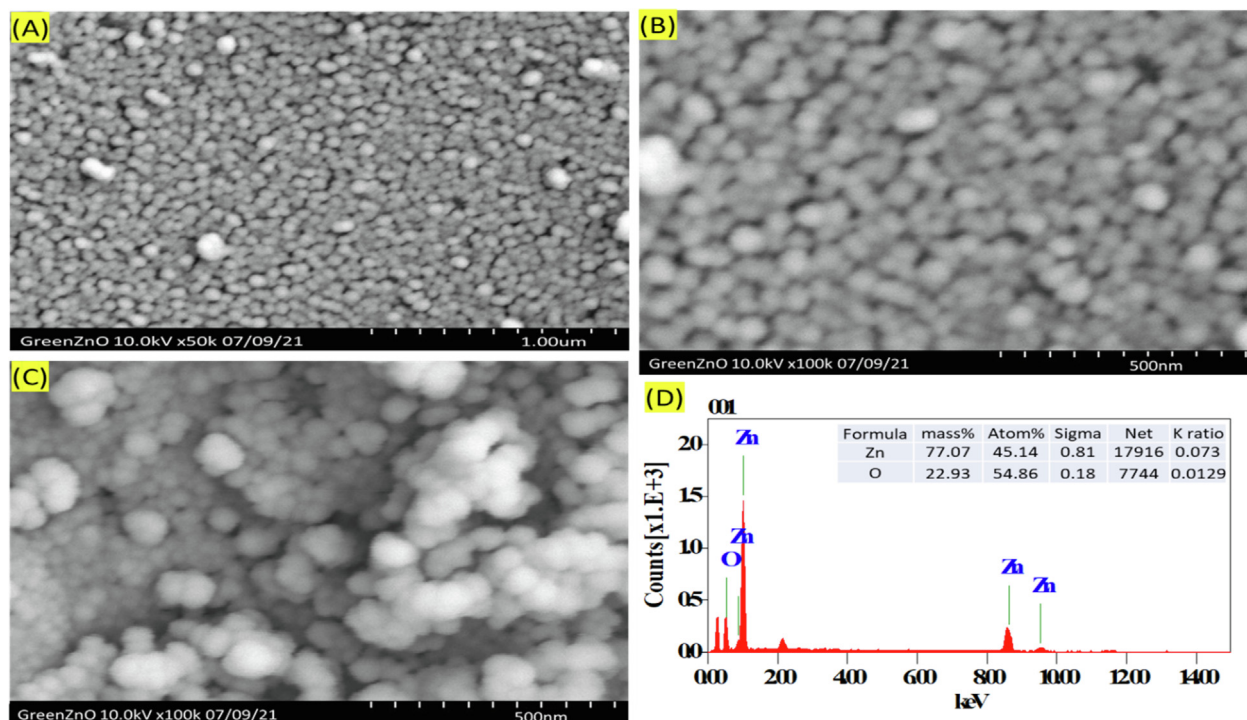
The high crystallinity of nanomaterials significantly increases the release of Zn<sup>2+</sup>, which interacts with the negatively charged cell membrane of bacteria through electrostatic interaction subsequently destruction of cell membrane and protein structure results in high antibacterial efficacy (Shuai et al., 2020).

### 3.4. Scanning electron microscope analysis (SEM)

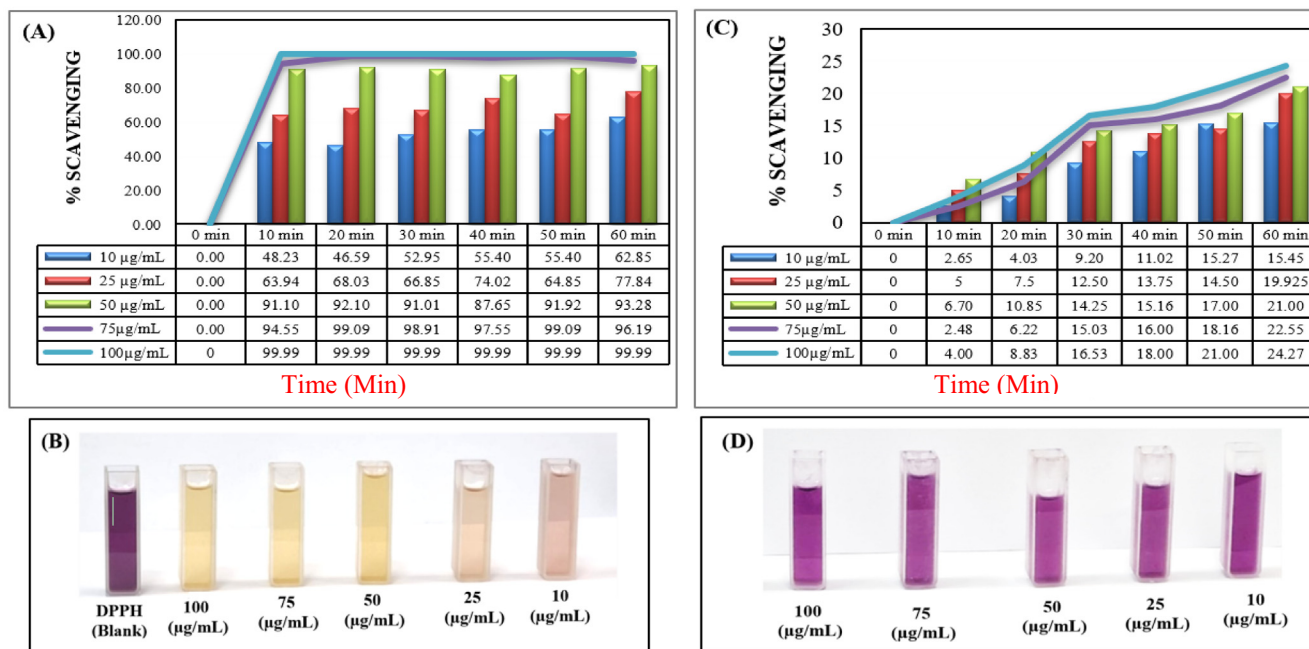
The surface morphology of the GsZnO-Nps was examined by using a scanning electron microscope having x50k and x100 k magnification. Fig. 5 (A, B, and C) shows monodispersed spherical particles of GsZnO-Nps having approximately 50 nm particle size as deduced from the cited scale. Fig. 5 (D) shows the energy-dispersive X-ray spectroscopy (EDS) analysis which reveals the quantitative elemental composition of GsZnO-Nps. The elemental analysis of green synthesis nanoparticles shows a mass % of Zn-77.07 and O- 22.93.

### 3.5. Anti-oxidant efficacy

Anti-oxidant efficacy of GsZnO-Nps and AR Grade ZnO were evaluated at different concentrations (10 to 100 µg/mL) by using nitrogen-centered free radical i.e. DPPH. The anti-oxidant efficacy of GsZnO-Nps and AR Grade ZnO was shown in Fig. 6 (A and C) up to 60 min. The systematic pictorial representation of scavenging of free radical color change due to GsZnO-Nps and AR Grade ZnO shown Fig. 6 (B and D). The free radical scavenging potency “FRSP” of



**Fig. 5** (A, B and C) Scanning Electron Microscopic images reveal the morphology of GsZnO-Nps shows spherical nanoparticles, (D) EDS of GsZnO-Nps revealing the elemental composition in graphical and tabulated form.



**Fig. 6** (A) anti-oxidant efficacy of GsZnO-Nps different concentration (10 to 100 µg/mL vs Time), (B) Pictorial representation anti-oxidant efficacy of GsZnO-Nps, (C) anti-oxidant efficacy of AR Grade ZnO, (D) Pictorial representation anti-oxidant efficacy of AR Grade ZnO given of comparison.

GsZnO-Nps at concentration 50, 75 and 100 µg/mL shows 91 % to 99.99 % after 30 min. However, FRSP of AR Grade ZnO was 14 % to 16 %. The IC<sub>50</sub> concentration of GsZnO-Nps was 21.72 µg/mL and AR Grade ZnO was 345.57 µg/

mL which is shown in Fig. 7 (A and B). The free radicle scavenging potency of GsZnO-Nps is significantly higher than in reported literature (Tetty and Shin, 2019). The high FRSP could be because of several reasons, influence of phytochemi-

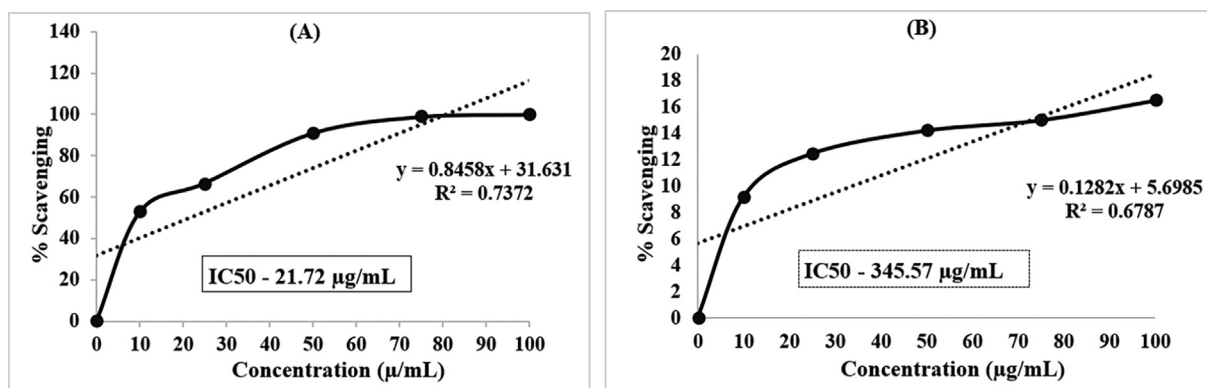


Fig. 7 IC<sub>50</sub> concentration (A) GsZnO-Nps and (B) AR Grade ZnO which is given for comparison.

cals of *Moringa oleifera* leaves extract and their bioactive attraction towards charged nanoparticles ( $\text{ZnO} = \text{Zn}^{2+} + \text{O}^{2-}$ ) which synergistically increase the bioactivity, formation of nanoscale particles, high specific surface area. The activity effects commonly depend on the attachment sites of the metals and their subsequent impact on the potency of the free radical scavenging (Kumar et al., 2014).

### 3.6. Anti-acne efficacy

The anti-acne efficacy of 0.0183 g/mL GsZnO-Nps and zinc acetate dihydrate was evaluated by disk diffusion technique against *C. acne* bacteria which is mainly responsible for causing acne on skin. The study was carried out in four different sets to minimize the experimental error. The average inhibition zone of GsZnO-Nps against *C. acne* was 33 mm having a standard deviation of 1.155 mm and a standard error of 0.557 mm. ZOI of zinc acetate dihydrate was 10.7 mm having a standard deviation of 0.559 mm and the standard error was 0.279 mm which is shown in Fig. 8 (A and B) and Table 2. The robust

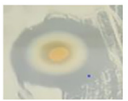
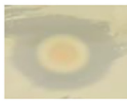

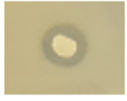
Figure	Sample details	Zone of inhibition in mm for <i>C. acne</i> ATCC 11827	
A	GsZnO-Nps (0.0183 g/mL)		
B	Zinc acetate dihydrate (0.0183 g/mL)		

Fig. 8 Representative images of anti-acne study against *C. acne* bacteria (A) ZOI of GsZnO-Nps (B) ZOI of Zinc acetate dihydrate salt.

anti-acne efficacy could be due to several reasons like the influence of active chemical constituents of *Moringa oleifera*, the particle size of metal oxide in nano regime, generation of reactive oxygen species, the release of  $\text{Zn}^{2+}$  ions which can rupture the micro-organism cell walls and potentially damage the internal organelle of the bacterial cell. The anti-acne efficacy is significantly higher than other reported literature (Bae and Park, 2016).

### 3.7. Anti-bacterial efficacy








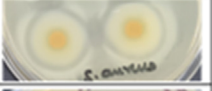


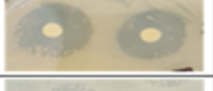





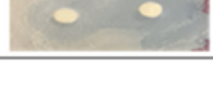
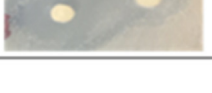
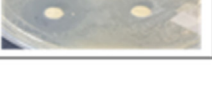
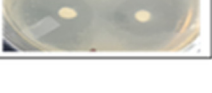
Anti-bacterial properties of GsZnO-Nps, AR Grade ZnO and standard drug were investigated by disk diffusion method. Different concentration like 10 µg/mL, 50 µg/mL, 100 µg/mL, 200 µg/mL of GsZnO-Nps, AR Grade ZnO and same for standard drugs used for the ZOI study against both Gram-positive (*S. aureus*) and Gram-negative (*E. coli*) pathogens which is shown in Fig. 9 (A and B). There is no inhibition zone observed in AR Grade ZnO. However, the higher concentration of GsZnO-Nps (200 µg/mL) have shown the average ZOI 26.75 mm against (*E. coli*) and 30.00 mm against (*S. aureus*). Standard drug (antibiotics) Doxycycline show the inhibition zone 24.0 mm and 22.5 mm against (*E. coli*) and 30.00 mm against (*S. aureus*), Azithromycin shows the strong inhibition zone against both (*E. coli*) and (*S. aureus*) respectively 31.00 mm and 30.00 mm as well as Cefpodoxime shows the inhibition zone approximately 20.25 mm and 19.75 mm against both (*E. coli*) and (*S. aureus*). The inhibition zone of GsZnO-Nps is directionally higher than standard drugs Doxycycline, Cefpodoxime and at par to Azithromycin inhibition zone at 200 µg/mL which is tabulated in Table 3. The anti-bacterial efficacy of GsZnO-Nps is significantly higher than reported literatures possibly due to influence of phytochemicals, high active specific surface area available for the interaction with microorganisms per unit mass, release of zinc ions,

Table 2 GsZnO-Nps anti-acne efficacy measured in inhibition zone against *C. acne*.



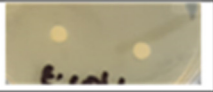

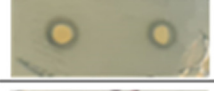






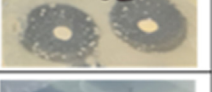


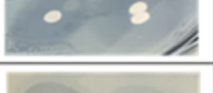

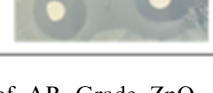
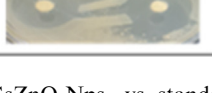
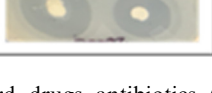
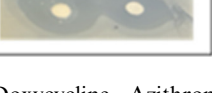
Sr. no.	Sample details	Zone of inhibition in mm for <i>C. acne</i> ATCC 11,827				Average	Std. deviation	Std. error
		Set 1	Set 2	Set 3	Set 4			
1	GsZnO-Nps (0.0183 g/mL)	34.00	34.00	32.00	32.00	33.00	1.155	0.577
2	Zinc acetate dihydrate (0.0183 g/mL)	11.1	10.5	10.00	11.2	10.70	0.559	0.279



**(A) Anti-bacterial efficacy against *S. aureus***

Concentration	10 µg/mL	50 µg/mL	100 µg/mL	200 µg/mL
AR Grade ZnO				
GsZnO-Nps				
Antibiotics- Doxycycline				
Antibiotics- Azithromycin				
Antibiotics- Cefpodoxime				

**(B) Anti-bacterial efficacy against *E. coli***

Concentration	10 µg/mL	50 µg/mL	100 µg/mL	200 µg/mL
AR Grade ZnO				
GsZnO-Nps				
Antibiotics- Doxycycline				
Antibiotics- Azithromycin				
Antibiotics- Cefpodoxime				

**Fig. 9** Anti-bacterial efficacy of AR Grade ZnO, GsZnO-Nps, vs standard drugs antibiotics (Doxycycline, Azithromycin and Cefpodoxime) against both Gram-positive and Gram-negative organism (A) *S. aureus* and (B) *E. coli*.

interaction of particles to cell membrane and generation of reactive oxygen species (Gupta et al., 2018).

### 3.8. Minimum inhibitory concentration

The MIC of GsZnO-Nps and AR Grade ZnO was determined against *E. coli* and *S. aureus* bacteria. MIC of GsZnO-Nps was found to be 500 µg/mL which is significantly lesser as to AR Grade ZnO (>900 µg/mL) shown in Table 4 which is in line with previous published literature (Ansari et al., 2012). Both, the inhibition zone and the MIC allow a prediction of therapeutic success. Concentration of GsZnO-Nps can be vary in both ZOI & MIC because while the MIC is a direct measurement of a concentration needed at the site of growth for bactericidal effect and the inhibition zone is that a given sample inhibits in whatsoever way the growth of the target bacterium and express bacteriostatic property (Ansari et al., 2012). Num-

ber of factors are responsible for anti-bacterial activity like reactive oxygen species (ROS), release of  $Zn^{2+}$  and direct contact of ZnO nanoparticles.

### 3.9. Possible mechanisms of anti-bacterial efficacy

Possible anti-bacterial mechanisms have been reported in the previous literatures such as: direct interaction of zinc oxide molecule with the bacterial cell wall and subsequently destructing the integrity of the cell (Brayner et al., 2006), release of  $Zn^{2+}$  ions (Cao et al., 2020), and generation of reactive oxygen species (ROS) (Lipovsky et al., 2011).

ROS are released due to photo-generated electrons and holes migrate to the active sites present at the surface of the nanomaterial. The holes being highly oxidizing will either oxidize the cell membrane directly or by forming strong hydroxyl radicals  $OH\cdot$  is an extremely powerful oxidizing agent that

**Table 3** Anti-bacterial efficacy measured in ZOI (mm) of AR Grade ZnO, GsZnO-Nps vs Standard drug.

Name of Test product	Conc. ( $\mu\text{g/mL}$ )	<i>E. coli</i> Inhibition Zone (mm)		<i>S. aureus</i> Inhibition Zone (mm)	
		Average	Std. dev.	Average	Std. dev.
AR Grade ZnO	10 $\mu\text{g/mL}$	0.00	0.00	0.00	0.00
	50 $\mu\text{g/mL}$	0.00	0.00	0.00	0.00
	100 $\mu\text{g/mL}$	0.00	0.00	0.00	0.00
	200 $\mu\text{g/mL}$	0.00	0.00	0.00	0.00
GsZnO-Nps	10 $\mu\text{g/mL}$	6.50	0.58	6.75	0.50
	50 $\mu\text{g/mL}$	14.50	1.73	14.25	0.96
	100 $\mu\text{g/mL}$	19.25	0.50	18.25	0.96
	200 $\mu\text{g/mL}$	26.75	1.50	30.00	1.83
Doxycycline	10 $\mu\text{g/mL}$	14.00	1.41	15.25	0.50
	50 $\mu\text{g/mL}$	18.25	0.96	17.75	1.89
	100 $\mu\text{g/mL}$	22.00	0.82	20.50	1.29
	200 $\mu\text{g/mL}$	24.00	1.83	22.50	1.73
Azithromycin	10 $\mu\text{g/mL}$	15.75	0.96	16.00	0.82
	50 $\mu\text{g/mL}$	21.75	0.50	22.25	0.96
	100 $\mu\text{g/mL}$	23.00	2.16	24.25	0.96
	200 $\mu\text{g/mL}$	31.00	1.41	30.00	1.41
Cefpodoxime	10 $\mu\text{g/mL}$	11.75	0.96	11.00	0.50
	50 $\mu\text{g/mL}$	15.00	1.83	16.25	0.96
	100 $\mu\text{g/mL}$	18.75	1.26	17.00	0.40
	200 $\mu\text{g/mL}$	20.25	0.96	19.75	0.96

**Table 4** MIC of GsZnO-Nps and AR Grade ZnO against both *E. coli* and *S. aureus* organism.

Material	Pathogen	Concentration ( $\mu\text{g/mL}$ )	Observation	MIC ( $\mu\text{g/mL}$ )
AR Grade ZnO	<i>E. coli</i>	900	Growth	> 900
		700	Growth	
		500	Growth	
		300	Growth	
		100	Growth	
	<i>S. aureus</i>	900	Growth	> 900
		700	Growth	
		500	Growth	
		300	Growth	
		100	Growth	
GsZnO-Nps	<i>E. coli</i>	900	No Growth	500
		700	No Growth	
		500	No Growth	
		300	Growth	
		100	Growth	
	<i>S. aureus</i>	900	No Growth	500
		700	No Growth	
		500	No Growth	
		300	Growth	
		100	Growth	

causes a partial or complete breakage of cell walls (Slavin et al., 2017).

It has also been reported that nanoparticle can release  $\text{Zn}^{2+}$  ions which potentially play a role in their anti-bacterial activities. Consequently, ion pathways and the dissociation of the plasma membrane allow ions to enter microbial cells (Song et al., 2010). Anaerobic metabolism and charge transfer

are inhibited, electrical activity and permeation are disturbed, and cell damage occurs as a result of  $\text{Zn}^{2+}$  ions reacting with thiol compounds of metabolic and transport proteins and lipids in the membrane. The  $\text{Zn}^{2+}$  shows the momentous effect in enzyme disruption, active transport inhibition, and amino acid metabolism (Aydin Sevinç and Hanley, 2010).

Direct interaction of ZnO due to the surface defect phenomenon and surface charge of ZnO nanoparticles play vital role for anti-bacterial mechanism. ZnO nanoparticles electrostatically interact and causing severe damage to the microbial cell wall. The surface morphology having rough and sharp topography leads to cell membrane damage (Schmidt-Mende and MacManus-Driscoll, 2007; Padmavathy and Vijayaraghavan, 2008). Furthermore, phytochemicals around GsZnO-Nps may also playing role to special features that impact bacterial cell walls and disrupt the structure of the cell membranes, resulting in lowered membrane potential and adenosine triphosphate generation. Phytochemicals produce changes in barrier function, metal ion chelate, and interruption in the function of membrane bound proteins, all of which alter the bacterial biological response and lead to death (AISheikh et al., 2020). Phenolic compounds have been shown to alter membrane structure and trigger the release of cell organelles, resulting in cell triphosphate deficiency (Gill and Holley, 2004).

#### 4. Conclusion

*Moringa oleifera* leaves extract is effectively used for the green synthesis of nanoscale ZnO. Fabrication of ZnO nanoparticles was confirmed using XRD, SEM, UV-vis analysis, and FT-IR studies. UV-vis spectra displayed the absorption band at 368.5 nm having band gap energy 3.36 eV has a blue shift in relation to AR grade ZnO. FT-IR spectrum

exhibits a characteristic peak of ZnO at 420 cm<sup>-1</sup>. SEM helps to examine the surface morphology of GsZnO-Nps having spherical particles evenly distributed having approximately 50 nm particle size as deduced from the cited scale. EDAX displayed the quantitative elemental analysis having 77.07 % zinc and 22.93 % oxygen element. The hexagonal wurtzite structure is shown through characteristic sharp peaks in XRD analysis, crystallite size is 13.82 nm calculated by using Debye Scherrer equation, high specific surface area 77.38 m<sup>2</sup>/g, and total crystallinity of 95.91 %. GsZnO-Nps has shown significantly high anti-oxidant activity having a half-maximal inhibitory concentration (IC<sub>50</sub>) of 21.72 µg/mL. Anti-oxidant activity is recommended to improve general health by helping to neutralize free radicals in our systems. Strong anti-acne efficacy established against *C. acne* bacteria which is mostly responsible for causing acne on skin, the average inhibition zone was 33.00 mm. GsZnO-Nps shows enhanced anti-bacterial activity having inhibition zone 26.75 mm and 30.00 mm against *E. coli* and *S. aureus* bacteria which is higher or equal to the standard drug while MIC of GsZnO-Nps was found to be 500 µg/mL which is much less when compared to AR Grade ZnO. Many fabrication methods present in the market. However, all are not allowed or compatible for personal care products due to their used precursor and byproduct. Therefore, there is still a lot to unleash in ZnO fabrication methodologies as well as selection of appropriate precursors suitable for health and hygiene products. Green based fabricated GsZnO-Nps shows high anti-bacterial and anti-oxidant efficacy which can be incorporated for multiple industrial applications like health and hygiene products, medicines and personal care applications such as anti-acne and anti-bacterial products (cream, lotion, face cleanser, soap bar, handwash, and bodywash etc.).

#### Declaration of Competing Interest

The authors declare that they have no known competing financial interests or personal relationships that could have appeared to influence the work reported in this paper.

#### Acknowledgements

Authors are highly thankful to IFFCO group, UAE, especially Mr. Isa Allana-Managing director (MD), Mr. Serhad C. Kelemci-Chief executive officer (CEO), Mr. Sunil Singh-Technical director, Sergey Michailovich Melnikov-Director-Oils, Fats & Culinary-R&D and NIT-Warangal's director for their encouragement and continuous support for this study.

#### References:

Abd El-Kader, M.F.H., Elabbasy, M.T., Adeboye, A.A., Zeariya, M. G.M., Menazea, A.A., 2021. Morphological, structural and antibacterial behavior of eco-friendly of ZnO/TiO<sub>2</sub> nanocomposite synthesized via *Hibiscus rosa-sinensis* extract. *J. Mater. Res. Technol.* 15, 2213–2220. <https://doi.org/10.1016/j.jmrt.2021.09.048>.

AlSheikh, H.M.A., Sultan, I., Kumar, V., Rather, I.A., Al-Sheikh, H., Tasleem Jan, A., et al, 2020. Plant-based phytochemicals as possible alternative to antibiotics in combating bacterial drug resistance. *Antibiotics* 9, 480. <https://doi.org/10.3390/antibiotics9080480>.

Ansari, M.A., Khan, H.M., Khan, A.A., et al, 2012. Synthesis and characterization of the antibacterial potential of ZnO nanoparticles against extended-spectrum β-lactamases-producing *Escherichia coli* and *Klebsiella pneumoniae* isolated from a tertiary care hospital of North India. *Appl. Microbiol. Biotechnol.* 94, 467–477. <https://doi.org/10.1007/s00253-011-3733-1>.

Anter, Abdelrhman & Awwad, Nasser. (2020). Antibacterial activity of TiO<sub>2</sub> doped ZnO composite synthesized via laser ablation route for antimicrobial application. *10.1016/j.jmrt.2020.05.103*.

Arya, V., 2010. Living systems: eco-friendly nanofactories. *Dig. J. Nanomater. Bios.* 5, 9–21.

Aydin Sevinç, B., Hanley, L., 2010. Antimicrobial activity of dental composites containing zinc oxide nanoparticles. *J. Biomed. Mater. Res. Part B: Appl. Biomater.* 9999B. <https://doi.org/10.1002/jbm.b.31620>.

Bae, J.Y., Park, S.N., 2016. Evaluation of anti-microbial activities of ZnO, citric acid and a mixture of both against *Propionibacterium acnes*. *Int. J. Cosmet. Sci.* 38 (6), 550–557. <https://doi.org/10.1111/ics.12318>.

Bechambi, O., Chalbi, M., Najjar, W., Sayadi, S., 2015. Photocatalytic activity of ZnO doped with Ag on the degradation of endocrine disrupting under UV irradiation and the investigation of its antimicrobial activity. *Appl. Surf. Sci.* 347, 414–420. <https://doi.org/10.1016/j.apsusc.2015.03.049>.

Behravan, M., Panahi, A.H., Naghizadeh, A., Ziaee, M., Mahdavi, R., Mirzapour, A., 2019. Facile green synthesis of silver nanoparticles using *Berberis vulgaris* leaf and root aqueous extract and its antimicrobial activity. *Int. J. Biol. Macromol.* 124, 148–154. <https://doi.org/10.1016/j.ijbiomac.2018.11.101>.

Bhalla, N., Athira, J.P., Ingle, N., Patel, H., Patri, S.V., Haranath, D., 2022. Fabrication and infusion of potent silver doped nano ZnO aimed to advance germicidal efficacy of health and hygiene products. *J. Sci.: Adv. Mater. Device.* <https://doi.org/10.1016/j.arabjc.2022.103862>.

Bhalla N., Ingle N., Srilakshmi V. Patri, D. Haranath, Phytochemical analysis of *Moringa oleifera* leaves extracts by GC-MS and free radical scavenging potency for industrial applications, Saudi Journal of Biological Sciences, Volume 28, Issue 12, 2021, Pages 6915-6928, ISSN 1319-562X, <https://doi.org/10.1016/j.sjbs.2021.07.075.C>.

Bhalla N., Ingle N., Patel H., Athira JP., Srilakshmi V. Patri, Ajeet Kaushik, D. Haranath, 2022. A Facile Approach to Fabricate and Embed Multifunctional Nano ZnO into Soap Matrix and Liquid Cleansing Products for Enhanced Antimicrobial and Photostability for Health and Hygiene Applications, Arabian Journal of Chemistry, 103862, ISSN 1878-5352, <https://doi.org/10.1016/j.arabjc.2022.103862>.

Biswas, B., Rogers, K., Mclaughlin, F., Daniels, D., Yadav, A., 2013. Antimicrobial activities of leaf extracts of Guava (*Psidium guajava* L.) on two gram-negative and Gram-positive bacteria. *Int. J. Microbiol.* <https://doi.org/10.1155/2013/746165>.

Brayner, R., Ferrari-Iliou, R., Brivois, N., Djediat, S., Benedetti, M.F., Fiévet, F., 2006. Toxicological impact studies based on *Escherichia coli* bacteria in ultrafine ZnO nanoparticles colloidal medium. *Nano Lett.* 6, 866–870. <https://doi.org/10.1021/nl052326h>.

Cao, D., Shu, X., Zhu, D., Liang, S., Hasan, M., Gong, S., 2020. Lipid-coated ZnO nanoparticles synthesis, characterization and cytotoxicity studies in cancer cell. *Nano Convergence* 7. <https://doi.org/10.1186/s40580-020-00224-9>.

Darroudi, M., Sabouri, Z., Oskuee, R.K., Zak, A.K., Kargar, H., Hamid, M.H.N.A., 2014. Green chemistry approach for the synthesis of ZnO nanopowders and their cytotoxic effects. *Ceram. Int.* 40, 4827–4831. <https://doi.org/10.1016/j.ceramint.2013.09.032>.

Debanath, M.K., Karmakar, S., 2013. Study of blueshift of optical band gap in zinc oxide (ZnO) nanoparticles prepared by low-temperature wet chemical method. *Mater. Lett.* 111, 116–119. <https://doi.org/10.1016/j.matlet.2013.08.069>.

Gill, A.O., Holley, R.A., 2004. Mechanisms of bactericidal action of cinnamaldehyde against *Listeria monocytogenes* and of eugenol against *L. monocytogenes* and *Lactobacillus sakei*. *Appl. Environ. Microbiol.* 70, 5750–5755.

Goktas, S., Goktas, A., 2021. A comparative study on recent progress in efficient ZnO based nanocomposite and heterojunction photo-

- catalysts: a review. *J. Alloy. Compd.* 863,. <https://doi.org/10.1016/j.jallcom.2021.158734> 158734.
- Gupta, M., Tomar, R.S., Kaushik, S., Mishra, R.K., Sharma, D., 2018. Effective antimicrobial activity of green ZnO nano particles of *Catharanthus roseus*. *Front. Microbiol.* <https://doi.org/10.3389/fmicb.2018.02030>.
- Halden, R.U., 2014. On the need and speed of regulating triclosan and triclocarban in the United States. *Environ. Sci. Tech.* 48, 3603–3611. <https://doi.org/10.1021/es500495p>.
- Hasan, M., Altaf, M., Zafar, A., Hassan, S.G., Ali, Z., Mustafa, G., Munawar, T., Saif, M.S., Tariq, T., Iqbal, F., Khan, M.W., Mahmood, A., Mahmood, N., Shu, X., 2021. Bioinspired synthesis of zinc oxide nano-flowers: a surface enhanced antimicrobial and harvesting efficiency. *Mater. Sci. Eng. C* 119,. <https://doi.org/10.1016/j.msec.2020.111280> 111280.
- Murtaza Hasan, Mahrukh Altaf, Ayesha Zafar, Shahbaz Gul Hassan, Zeeshan Ali, Ghazala Mustafa, Tauseef Munawar, Muhammad Saqib Saif, Tuba Tariq, Faisal Iqbal, Muhammad Waqas Khan, Asif Mahmood, Nasir Mahmood, Xugang Shu, Bioinspired synthesis of zinc oxide nano-flowers: A surface enhanced antibacterial and harvesting efficiency, *Materials Science and Engineering: C*, Volume 119, 2021, <https://doi.org/10.1016/j.msec.2020.111280>
- Hasnidawani, J.N., Azlina, H.N., Norita, H., Bonnia, N.N., Ratim, S., Ali, E.S., 2016. Synthesis of ZnO nanostructures using sol-gel method. *Procedia Chem.* 19, 211–216. <https://doi.org/10.1016/j.proche.2016.03.095>.
- Iqbal, J., Abbasi, B.A., Yaseen, T., et al, 2021. Green synthesis of zinc oxide nanoparticles using *Elaeagnus angustifolia L.* leaf extracts and their multiple in vitro biological applications. *Sci. Rep.* 11, 20988. <https://doi.org/10.1038/s41598-021-99839-z>.
- Iravani, S., 2011. Green synthesis of metal nanoparticles using plants. *Green Chem.* 13, 2638–2650. <https://doi.org/10.1039/C1GC15386B>.
- Jayachandran, A., Aswathy T.R., Achuthsankar S. Nair, 2021. Green synthesis and characterization of zinc oxide nanoparticles using *Cayratia pedata* leaf extract, *Biochemistry and Biophysics Reports*, Volume 26, 100995, ISSN 2405-5808, <https://doi.org/10.1016/j.bbrep.2021.100995>
- Jianrong, M. Yuqing, H. Nongyue, W. Xiaohua, L. Sijiao, *Nanotechnology and biosensors*, *Biotechnol. Adv.* 22 (2004) 505–518, <https://doi.org/10.1016/j.biotechadv.2004.03.004>
- Joshi, R., Sathasivam, R., Park, S.U., Lee, H., Kim, M.S., Baek, I., Cho, B.-K., 2022. Application of fourier transform infrared spectroscopy and multivariate analysis methods for the non-destructive evaluation of phenolics compounds in Moringa powder. *Agriculture* 12 (1), 10. <https://doi.org/10.3390/agriculture12010010>.
- Kalpana, V.N., Rajeswari, V.D., 2018. A review on green synthesis, biomedical applications, and toxicity studies of ZnO NPs. *Bioinorg. Chem. Appl.* <https://doi.org/10.1155/2018/3569758>.
- Kolekar, T.V., Bandgar, S.S., Shirguppikar, S.S., Ganachari, V.S., 2013. Synthesis and characterization of ZnO nanoparticles for efficient gas sensors. *Arch. Appl. Sci. Res.* 5, 20–28.
- Kołodziejczak-Radzimska, A., Jesionowski, T., 2014. Zinc oxide— from synthesis to application: a review. *Materials* 7, 2833–2881. <https://doi.org/10.3390/ma7042833>.
- Kumar, B., Kumari, S., Luis, C., Alexis, D., 2014. Green approach for fabrication and applications of zinc oxide nanoparticles. *Bioinorg. Chem. Appl.* 1–7. <https://doi.org/10.1155/2014/523869>.
- Lamore, S.D., Cabello, C.M., Wondrak, G.T., 2010. The topical antimicrobial zinc pyrithione is a heat shock response inducer that causes DNA damage and PARP-dependent energy crisis in human skin cells. *Cell Stress Chaperones* 15, 309–322. <https://doi.org/10.1007/s12192-009-0145-6>.
- Lei, Y., Qu, F., Wu, X., 2012. Assembling ZnO nanorods into microflowers through a facile solution strategy: morphology control and cathodoluminescence properties. *Nano-Micro Lett.* 4, 45–51. <https://doi.org/10.1007/bf03353691>.
- Lipovsky, A., Nitzan, Y., Gedanken, A., Lubart, R., 2011. Antifungal activity of ZnO nanoparticles—the role of ROS mediated cell injury. *Nanotechnology* 22,. <https://doi.org/10.1088/0957-4484/22/10/105101> 105101.
- Makarov, V.V. et al, 2014. “Green” nanotechnologies: synthesis of metal nanoparticles using plants. *Acta Nat.* 6, 35–44.
- Malik, P., Shankar, R., Malik, V., Sharma, N., Mukherjee, T.K., 2014. Green chemistry based benign routes for nanoparticle synthesis. *J. Nanopart.* <https://doi.org/10.1155/2014/302429>.
- Menazea, A.A., Ismail, A.M., Samy, A., 2021. Novel green synthesis of zinc oxide nanoparticles using orange waste and its thermal and antibacterial activity. *J. Inorg. Organomet. Polym.* 31, 4250–4259. <https://doi.org/10.1007/s10904-021-02074-2>.
- Moodley, J.S., Krishna, S.B.N., Pillay, K., Govender, P., 2018. Green synthesis of silver nanoparticles from *Moringa oleifera* leaf extracts and its antimicrobial potential. *Adv. Nat. Sci. Nanosci. Nanotechnol.* 9, 015011.
- Nadagouda, M.N., Varma, R.S., 2008. Green synthesis of silver and palladium nanoparticles at room temperature using coffee and tea extract. *Green Chem.* 10, 859–862. <https://doi.org/10.1039/B804703K>.
- Oprea, O., Andronescu, E., Vasile, B., Voicu, G., Covaliu, C., 2011. Synthesis and characterization of ZnO Nano powder by non-basic route. *Digest J. Nanomater. Biostruct.* 6, 1393–1401.
- Padmavathy, N., Vijayaraghavan, R., 2008. Enhanced bioactivity of ZnO nanoparticles—an antimicrobial study. *Sci. Technol. Adv. Mater.* 9,. <https://doi.org/10.1088/1468-6996/9/3/035004> 035004.
- Phoohinkong, W., Foophow, T., Pecharapa, W., 2017. Synthesis and characterization of copper zinc oxide nanoparticles obtained via metathesis process. *Adv. Nat. Sci. Nanosci. Nanotechnol.* 8, (3). <https://doi.org/10.1088/2043-6254/aa7223> 035003.
- P. Rajiv, S. Rajeshwari, R. Venkatesh, Bio-Fabrication of zinc oxide nanoparticles using leaf extract of *Parthenium hysterophorus L.* and its size-dependent antifungal activity against plant fungal pathogens, *Spectrochim. Acta Mol. Biomol. Spectrosc.* 112 (2013) 384–387, <https://doi.org/10.1016/j.saa.2013.04.072>
- Sánchez-Martín, S., Olaizola, S.M., Castaño, E., Urionabarrenetxea, E., Mandayo, G.G., Ayerdi, I., 2021. Study of deposition parameters and growth kinetics of ZnO deposited by aerosol assisted chemical vapor deposition. *RSC Adv.* 11, 18493–18499. <https://doi.org/10.1039/d1ra03251h>.
- Schmidt-Mende, L., MacManus-Driscoll, J.L., 2007. ZnO – nanostructures, defects, and devices. *Mater. Today* 10, 40–48. [https://doi.org/10.1016/s1369-7021\(07\)70078-0](https://doi.org/10.1016/s1369-7021(07)70078-0).
- Shuai, C., Wang, C., Qi, F., Peng, S., Yang, W., He, C., Wang, G., Qian, G., 2020. Enhanced crystallinity and antimicrobial of PHBV scaffolds incorporated with zinc oxide. *J. Nanomater.* 1–12. <https://doi.org/10.1155/2020/6014816>.
- Siddiqi, K.S., ur Rahman, A., Tajuddin et al. Properties of Zinc Oxide Nanoparticles and Their Activity Against Microbes. *Nanoscale Res Lett* 13, 141 (2018). <https://doi.org/10.1186/s11671-018-2532-3>
- Singh, M., Singh, S., Prasad, S., Gambhir, I.S., 2008. Nanotechnology in medicine and antimicrobial effect of silver nanoparticles. *Dig. J. Nanomater. Bios.* 3, 115–122.
- Singh, Tejasvi, et al. “Green Synthesized Gold Nanoparticles with Enhanced Photocatalytic Activity.” *Materials Today: Proceedings*, vol. 42, 2021, pp. 1166–1169, 10.1016/j.matpr.2020.12.531.
- Slavin, Y.N., Asnis, J., Häfeli, U.O., et al, 2017. Metal nanoparticles: understanding the mechanisms behind antimicrobial activity. *J. Nanobiotechnol.* 15, 65. <https://doi.org/10.1186/s12951-017-0308-z>.
- Song, W., Zhang, J., Guo, J., Zhang, J., Ding, F., Li, L., Sun, Z., 2010. Role of the dissolved zinc ion and reactive oxygen species in cytotoxicity of ZnO nanoparticles. *Toxicol. Lett.* 199, 389–397. <https://doi.org/10.1016/j.toxlet.2010.10.003>.
- J. Suresh, G. Pradheesh, V. Alexramani, M. Sundrarajan, S.I. Hong, Green synthesis and characterization of zinc oxide nanoparticle using insulin plant (*Costus pictus D. Don*) and investigation of its

- antimicrobial as well as anticancer activities, *Adv. Nat. Sci. Nanosci. Nanotechnol.* 9 (2018), 015008, <https://doi.org/10.1088/2043-6254/aaa6f1>.
- Sushma, N.J., Mahitha, B., Mallikarjuna, K., Deva, P.R.B., 2016. Bio-inspired ZnO nanoparticles from "*Ocimum tenuiflorum*" and their in vitro antioxidant activity. *Appl. Phys. A* 122, 544.
- Tetty, C.O., Shin, H.M. 2019. Evaluation of the antioxidant and cytotoxic activities of zinc oxide nanoparticles synthesized using *scutellaria baicalensis* root, *Scientific African*, Volume 6, e00157, ISSN 2468-2276, <https://doi.org/10.1016/j.sciaf.2019.e00157>
- Vasile, O.-R., Andronescu, E., Ghitulica, C., Vasile, B.S., Oprea, O., Vasile, E., Trusca, R., 2012. Synthesis and characterization of nanostructured zinc oxide particles synthesized by the pyrosol method. *J. Nanopart. Res.* 14. <https://doi.org/10.1007/s11051-012-1269-7>.
- Virkutyte, J., Varma, R.S., 2011. Green synthesis of metal nanoparticles: biodegradable polymers and enzymes in stabilization and surface functionalization. *Chem. Sci.* 2, 837–846. <https://doi.org/10.1039/C0SC00338G>.
- Wirunchit, S., Gansa, P., Koetnyom, W., 2021. Synthesis of ZnO nanoparticles by Ball-milling process for biological applications. *Materials Today: Proceedings*. <https://doi.org/10.1016/j.matpr.2021.03.559>.
- Yedurkar, S., Maurya, C., Mahanwar, P., 2016. Biosynthesis of zinc oxide nanoparticles using *ixora coccinea* leaf extract—a green approach. *Open J. Synth. Theor. Appl.* 5, 1. <https://doi.org/10.4236/ojsta.2016.51001>.
- Zhang, X., Guo, Q., Cui, D., 2009. Recent advances in nanotechnology applied to biosensors. *Sensors* 9, 1033–1053. <https://doi.org/10.3390/s90201033>.
- Zheng, Z.Q., Yao, J.D., Wang, B., Yang, G.W., 2015. Light-controlling, flexible and transparent ethanol gas sensor based on ZnO nanoparticles for wearable devices. *Sci. Rep.* 5, 1107. <https://doi.org/10.1038/srep11070>.